PHYSICAL REVIEW A VOLUME 22, NUMBER 3 SEPTEMBER 1980

# Laser magnetic resonance spectroscopy of normally forbidden transitions: Electrostatic fine structure of the $n=9, L=1$–$8$ $^4$He singlet states

R. Panock,*† M. Rosenbluh, and B. Lax†
*Francis Bitter National Magnet Laboratory, Massachusetts Institute of Technology, Cambridge, Massachusetts 02139*

Terry A. Miller‡
*Bell Laboratories, Murray Hill, New Jersey 07974*
(Received 29 February 1980)

Forbidden transitions have been observed from the $7\,^1S$ state of $^4$He to the manifold of states, $n=9$, $L=1$–$8$. These transitions are tuned into resonance with $CO_2$ laser lines by an applied magnetic field of 0–140 kG. Transitions to the odd-parity states are characterized by a velocity-dependent, motional Stark effect line shape which has been described previously. Transitions to the even-parity states have, in addition, a velocity-dependent transition moment creating a more complex line shape whose form is derived in an adjoining article. Analysis of the positions of over 20 observed resonances allows a determination of the zero-field separations of all the $n=9$, $L=1$–$8$ states of He, and the quantum defects for He singlet states with $L>0$.

## I. INTRODUCTION

Through the use of moderate laser powers and a unique combination of magnetic and motional Stark-electric fields, we have observed a large number of normally "forbidden" transitions in the pentultimately simplest atom He. In several previous publications[1-4] we reported our measurements of the electrostatic and relativistic fine structure of several highly excited Rydberg states of $^4$He. In Ref. 2 we described our observation of the allowed $7\,^1S$-$9\,^1P$ transitions. Also presented in that paper were a description of the apparatus, the methods used and a full analysis of the unusual motional Stark effect (MSE) line shape associated with these transitions. In Ref. 4 we presented our initial observations of laser driven forbidden transitions originating in the $7\,^1S$ state and ending in all the even-parity, $m_L=+2$, states with principal quantum number $n=9$. The essential features of a new velocity-dependent line shape, associated with these forbidden transitions, was also presented there.

In this paper we report results obtained from a full set of $CO_2$ laser-driven transitions between the $7\,^1S$ and the $n=9$, even-parity, $m_L=+2$ set of states, obtained in magnetic fields ranging from 20–140 kG. In addition, we also present the results obtained from our observation of transitions between the $7\,^1S$ state and the $n=9$, odd-parity, $m_L=+1$ set of states. A detailed analysis of the mechanisms responsible for the breakdown of the normal selection rules, and the line shapes applicable to these transitions are presented in an adjoining paper.[5] We obtain new and accurate electrostatic fine-structure intervals for the $n=9$, $L=1$–$8$, $^4$He singlet states, by extrapolating our results to zero magnetic field through the use of an accurate higher order Zeeman tuning theory.

The fine structure of He, both electrostatic and relativistic has been the subject of numerous high precision spectroscopic experiments in the past 20 years.[6,7] Early work centered on the lowest excited states, with the metastable $2\,^3S$ level being studied by Hughes and co-workers[8-10] by the molecular beam magnetic resonance method, and the $n=2$, $3\,^3P$ states being studied by Lamb and coworkers[11-14] by the microwave optical double resonance method. The latter technique was later extended[15,16] to the $n=4$, $5\,^3P$ He states by Miller and Freund and then used extensively first by Wing and Lamb[17-19] then by Wing, MacAdam and coworkers[7,20-23] to characterize a number of $n$, $L$ ($L\leq 4$) states. During the same period anticrossing spectroscopy was used[24-28] to characterize the interactions and separations of the $n=3$–$20\,^1D$ and $^3D$ states of He.

Our method[1,2] has extended the optical microwave resonance technique into the IR by replacing the microwave oscillator with a $CO_2$ laser. In order to have a magnetic tuning range large compared to separations of the fixed frequency $CO_2$ laser lines we have employed a high homogeneity Bitter solenoid with a field capability of ~140 kG. This technique has allowed the high precision (<0.1 ppm) measurement of He intervals, e.g., $7\,^1S$-$9\,^1P$, inaccessible to other techniques. It has also, perhaps more importantly, opened the subject of the behavior of atomic levels in intense magnetic fields to the probing of precision spectroscopy.

Considerable theoretical interest[29-33] has been shown in both the subject of the energy levels of He and atomic behavior in high magnetic fields.[34] Chang and Poe[30,32] have done extensive calculations of He fine structure and in general obtained agree-

 

ment with experiment to the level of 1–2%. Recent calculations[33] on He fine structure claim to reduce the above discrepancy by a factor of ~5.

After the work of Farley *et al.*[7] the lower ($2 \leq L \leq 4$) $L$ fine structure of He is vastly better known than for higher $L$. Indeed only one other experiment[35] has previously observed and clearly resolved high-$L$ states. This involved anticrossing observations between high-$L$ states and the $^{1,3}D$ state. These anticrossings were induced by an external electric field perpendicular to the magnetic field. Results were obtained for $n=7$–11 and $4 \leq L \leq 7$. Electrostatic fine-structure measurements of low-$L$ He states ($L \leq 3$) using far IR lasers is discussed elsewhere.[36]

In our experiments we observe clearly resolved transitions to all existing $L$ states in the absence of any applied external electric field. Our ability to drive these transitions is a consequence of the breakdown of the normal selection rules by two different effects of an intense field. The first is the mixing of states of the same parity and magnetic projection quantum number, $m_L$, by the diamagnetic part of the Zeeman Hamiltonian. This mixes $^1P$ character (with its allowed $\Delta L=1$, $\Delta m_L=1$ transition probability) into the singlet $L=3$, 5, and 7 states. The second effect of the magnetic field is to cause an atom moving through it to "see" a "motional" electric field. This electric field mixes $^1P$ character into the $^1D$ state from which it is propagated to the $L=4$, 6, 8 states by the diamagnetic interaction.

As we have shown previously,[1-4] the MSE is dependent upon the atom's velocity and it combines with the Doppler effect to produce new and very interesting line-shape effects. The transitions to the $n=9$, odd-parity states exhibit the MSE line shapes as described before. The transitions to the even-parity states, however, depend upon this same MSE for their transition probability. This gives rise to a velocity-dependent transition moment which complicates the line-shape function. A further complexity arises when one includes the effects of laser power saturation into the calculation, as this too is velocity dependent. All of these velocity-dependent effects are taken into account in the line-shape derivation presented in the previous paper.[5]

By employing this line-shape analysis, the centers of all the observed resonances involving the high-$L$ states are determined and then globally fit to obtain the best zero-field separations for all the levels of the $n=9$ manifold, $L=1$ to 8. The present analysis of moderately high Rydberg levels studied with very high resolution nicely complements recent studies[37-44] of higher Rydberg states in magnetic fields with lower spectral resolution. Such studies are of considerable current theoretical interest.[45-47]

## II. EXPERIMENTAL APPARATUS

As we have previously described our experimental apparatus,[1,2,4] we limit ourselves to a brief account. The excited states of helium are differentially populated by electron bombardment. The vacuum chamber containing the electron gun and helium gas is located in the bore of a feedback stabilized Bitter electromagnet, which provides a field from 0 to 140 kG. Absolute field measurements are made with a wide band NMR gaussmeter. A fixed frequency, step-tunable $CO_2$ laser is used to drive transitions between excited states of the helium atoms. The population in an excited state is monitored by observing the uv-visible fluorescence from that state to a lower lying one. In these experiments, we monitored the $7\,^1S$-$2\,^1P$ fluorescence at 4024 Å as a function of magnetic field.

Since all the transitions described here are in zeroth-order forbidden, to make them observable in a reasonable amount of time we operated the laser at higher power and the electron gun at slightly higher currents than previously.[2] The laser frequency was inferred by tuning the cavity length to maximize the output power. Under the high gain, high power conditions used in this experiment, the uncertainty of the laser frequency varied from 6–17 MHz. For the majority of the measurements the electron current was increased from the normal[2] 1 to 3 mA. No noticeable change in the resonance positions were observed when the current was so increased but a significant increase in signal was obtained. The gas pressure as measured by a capacitance manometer was ~15 mTorr.

## III. EXTERNAL FIELD PERTURBATIONS ON THE $n=9$ He STATES

In the preceding article[5] we presented a general method of dealing with the effect of the intense magnetic field upon the energy levels and transition probabilities of an atomic system. We now apply these general results to the $n=9$ singlet states of He for which we have experimental data.

In Fig. 1 we show the energy level diagram for several He singlet states in the vicinity of $n=9$. From this figure we can immediately see that the $n=9$ manifold is very well isolated and thus the exclusion of the $n=8$ and $n=10$ states from the diagonalization of the full Zeeman Hamiltonian is justified. Also shown in the figure is the hydrogenic energy level for $n=9$. The very close proximity of all the $n=9$ He states with $L>0$ to this

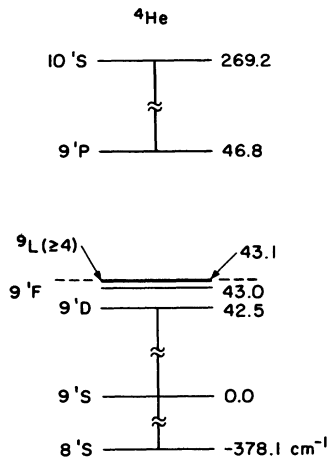


FIG. 1. Schematic diagram showing approximate, zero-field energy level structure for some states relevant to the experiment. The energies indicated are in $cm^{-1}$. The dashed line indicates the hydrogenic energy for $n=9$.

hydrogenic energy is the justification for our use of hydrogenic wave functions. In fact the quantum defects of He, $\delta(L)$, for all states with $L>0$ are very small, with the largest being $\delta(^1P)=-0.012$.

As we noted above the magnetic field can only mix states with $\Delta L=0,\pm2$ and $\Delta m_L=0$, so we need only consider states with the same values of $m_L$ and the same parity. This greatly simplifies the numerical problem of diagonalizing the full Hamiltonian. For example, the matrix to be diagonalized for the $m_L=+2$ even-parity states is only four by four as is the one for the $m_L=+1$ odd-parity states. We will consider these two cases in particular ($m_L=+2$—even parity and $m_L=+1$—odd parity) since our data was obtained for these two sets of states.

In Figs. 2 through 5 we show the results for the Zeeman diagonalization using the zero-field energies from Refs. 7 and 35. In Figs. 2 and 3 we show the Zeeman tuning of the energy levels for fields from 0 to 140 kG. A linear Zeeman tuning term of $\mu_0 B$ in Fig. 2 and $2\mu_0 B$ in Fig. 3 is substracted from the energies shown, in order to more clearly show the nonlinear behavior of the Zeeman tuning. Figure 3 for the even-parity states also shows the tuning of the $^1P$, $m_L=+1$ state, since this state will be pertinent to our later discussion. The dots in Figs. 2 and 3 indicate the fields at which the laser-driven resonances were observed.

A very important result of the diagonalization is the new set of eigenvectors [as given by Eq. (3) in the preceding paper] that characterize the states at a particular value of the magnetic field. In Figs. 4 and 5 we show the coefficients, $|C(L_0,m_L,L)|^2$, from this equation, as a function of magnetic

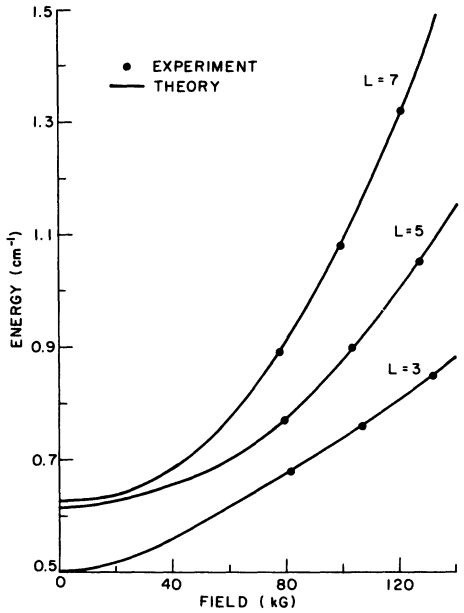


FIG. 2. The energies (minus $\mu_0 H$) of the odd-parity, $m_L=1$ states as a function of magnetic field. Solid circles indicate fields at which resonances were observed.

field for the various $L$ states in our example. These coefficients are physically very significant since they represent the amount of zero-field $|L,m_L\rangle$ character that a state $|L_0,m_L\rangle$ has at a particular value of $B$. Since the transitions from the $7\,^1S$ state to the odd-parity states become allowed in proportion to the amount of $^1P$ character mixed into them, the vertical axis in Fig. 4 is directly proportional to the transition moment, or the ease of driving a transition to that state.

The transitions to the even-parity states take place because of the magnetic mixing of these states with the $^1D$ state, which in turn contains

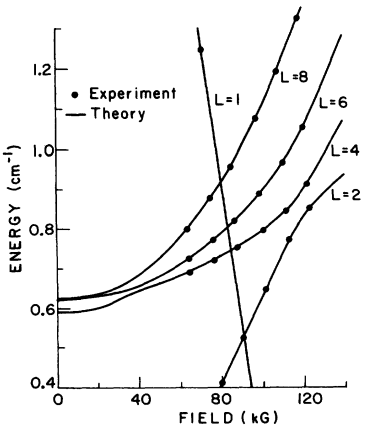


FIG. 3. The energies (minus $2\mu_0 H$) of the even-parity (and $^1P$, $m_L=1$), $m_L=2$ states as a function of magnetic field. Solid circles indicate fields at which resonances were observed.

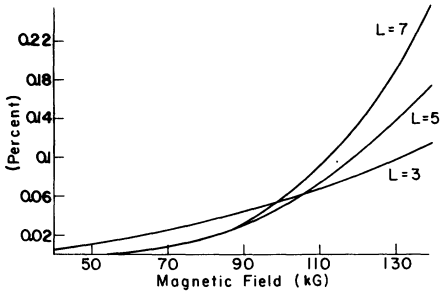


FIG. 4. Admixture of $^1P$ character in the singlet, odd-parity, $m_L=1$ states as a function of magnetic field.

some electric field-induced $^1P$ character. Thus the admixture of $^1D$ character, as shown in Fig. 5 for the even-parity states is but one of the determining factors in the transition moments to these states. The motional electric field mixes the states with $\Delta L=\pm1$, $\Delta m_L=\pm1$. To first order the electric field only mixes $^1P$ character into the $^1S$ and $^1D$ states, and the $^1S$ state lies too far away from all the other $L$ states to significantly interact with them. The $^1D$ state can, however, interact with the high-$L$ states via the magnetic mixing of states of the same even parity.

As we noted in the previous paper,[5] we account for the motional electric field using perturbation theory. The one place that this simple treatment could break down is near the anticrossings of the $9\,^1P$, $m_L=1$ and $9\,^1L$, $m_L=2$ states as shown in Fig. 3. We have performed a more detailed treatment of the electric field perturbation here by diagonalizing exactly the relevant two-state matrices. However, the results are not particularly significant as we have no data near the anticrossing. This procedure, however, assures us that elsewhere, the perturbation approach is well justified.

The perturbational procedure for calculating the $9\,^1P$, $m_L=+1$ character of the even parity, $m_L=+2$ states obtained from the diagonalization is straightforward. We first compute the electric field mixing coefficients of a particular even-parity state with each of the odd-parity $m_L=+1$ states, as given by Eq. (6) of the previous paper. We then multiply each mixing coefficient by the amount of $9\,^1P$, $m_L=+1$ character in the corresponding odd-parity, $m_L=+1$ state, shown in Fig. 4, and sum the results. This total amount of $9\,^1P$, $m_L=1$ character for a thermal velocity atom with $T=450$ K, is shown in Fig. 6 as a function of magnetic field.

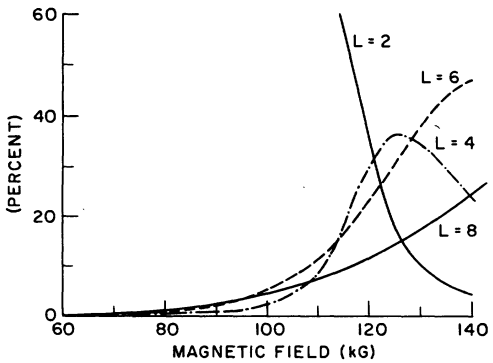


FIG. 5. Admixture of $^1D$ character in the singlet, even-parity, $m_L=2$ states as a function of magnetic field.

## IV. DATA ANALYSIS

As shown in Fig. 3, the high-$L$, $m_L=2$, even-parity transitions were observed with several laser lines at various fields above about 65 kG. (The transitions to the $9\,^1D$ state were actually observed at fields as low as 20 kG, although the lower field points are not indicated in the figure.) The lowest field at which transitions were observed to the high-$L$, odd-parity, $m_L=1$ states, is between 75–82 kG as shown in Fig. 2. Since these states are relatively weakly coupled to the $9\,^1P$ (as can be seen from Fig. 4), transitions to them at fields below 75 kG are not easily observable.

In order to facilitate the discussion of all these transitions we organize this section as follows: We first discuss the parameters that have a bearing on the observed transitions and line shapes. This includes the various velocity-independent broadening mechanisms (lifetime, collision, laser power, electric and magnetic field inhomogeneities). The method used to determine the gas temperature which also plays a key role in the line shape is discussed next. We then discuss the line-shape fitting details for the various transitions. This section concludes with the extrapolations to zero magnetic fields and the determination of the zero-field energies of the states.

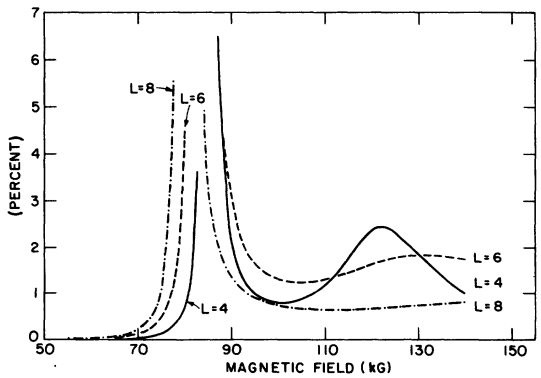


FIG. 6. Electric field-induced admixture of $^1P$ character in the singlet $n=9$, $L=4$, 6, 8 states, as a function of magnetic field, for an atom moving with velocity $v_0$, for $T=450$ K.

### A. Parameters pertaining to the data

#### 1. Lifetime width

There are several different characteristic times that can be important in determining the dominant mechanism (if there exists one) for lifetime broadening. The lifetime of a state can be governed either by collisional or radiative decay and the collisional lifetime can be dominated either by elastic or inelastic collisions. To get an estimate of the collisional lifetime we calculate the mean collision time. This is just given by

$$\tau_c = 1/nv_0\sigma,$$

where $n$ is the density of atoms, $v_0$ is the previously defined[5] mean thermal velocity, and $\sigma$ is taken to be the geometrical cross section, $\pi\langle r^2\rangle$. At a pressure of 15 microns and a temperature of 450 K the above expression yields a lifetime of 132 ns for the $7\,^1S$ and 49 ns for the $9\,^1P$ state.

In a simplistic theory it is difficult to determine how many of these collisions are elastic and how many are inelastic. We are, in any case, quite sure that collisional depopulation of a state is possible because there are many states nearby the states of interest. There have been measurements of collisional angular momentum transfer in both helium and other Rydberg atoms.[48,49] Indications are that for $n$ values $\lesssim 7$, experimental $\Delta L$ changing cross sections for high $L$ seem to fit calculated geometrical cross sections. However, for $n$ values $\gtrsim 7$, in spite of the larger size of the electron orbital, the cross section levels off. A reasonable estimate for a collisional cross section with a neutral atom can vary from the geometrical cross section to an order of magnitude smaller. In our system there also exist free ions and electrons which we have not taken into account. Even though we do not include the effect of these species on the lifetime of the states, their effect is certainly to further shorten it. We proceed under the assumption that the collisional lifetime is given by the geometrical cross section. The consequences of this uncertainty are discussed later.

The radiative lifetimes for states in helium have been calculated for states up to $8\,^1P$ and we have extrapolated a result for the $9\,^1P$ state.[50] We find that the $7\,^1S$ lifetime is 356 ns and that of the $9\,^1P$ state is 41 ns. Thus a reasonable estimate for $T_2$, the previously defined phase coherence time,[5] for a transition to a high-$L$ state with $n=9$ is ~30 ns (assuming that high-$L$ states have very long radiative lifetimes and their collisional lifetime is about 50 ns). This corresponds to a full width at half maximum (FWHM) $\sim 2\times 10^{-4}$ cm$^{-1}$ or ~7 G for $m_L=1$, and ~3 G for $m_L=2$ states.

#### 2. Power broadening

The quantity we are interested in calculating is $I_{SO}$ as given by Eq. (12) of the previous paper. We recall $M^0_{um}$ in Eq. (12) of the previous paper is the amount of $^1P$, $m_L=+1$ character in the high-$L$ state. The quantity $\mu_{im}$ is the transition moment for the allowed transition between the $7\,^1S$, $m_L=0$ and $9\,^1P$, $m_L=+1$ states in our case. It is given by

$$\mu_{im} = e\langle i|x|f\rangle = e\langle 7,0,0|r\sin\theta\cos\phi\,|9,1,1\rangle = 3.42ea_0, \quad (1)$$

where the angular integral is obtained analytically and the radial integral numerically.[51] The only other quantities appearing in Eq. (12) of the previous paper for $I_{SO}$ are $T_2$ and $\tau$, which for high-$L$ states we have shown to be about equal, $T_2=\tau=30$ ns, since the radiative lifetime of these states is very long. Combining all of these quantities we obtain that $I_{SO}\approx 1.7/M^0_{um}$ (mW/cm$^2$).

Our previous experience with the $7\,^1S$-$9\,^1P$ transition led us to believe that this value of $I_{SO}$ was about a factor of 2 too small when compared with values obtained experimentally for laser powers measured outside the chamber. This discrepancy is attributed to the difficulty in measuring the laser intensity that actually arrives at the interaction region with the appropriate polarization. Even a slight optical misalignment can rotate the polarization vector of the beam. Based upon our previous experience,[51] therefore, we adopted a semiempirical saturation intensity of $\approx 3.8/M^0_{um}$ (mW/cm$^2$) in our line fitting.

The weak link in the line fitting parametrization is the calculation of saturation intensity and lifetime for the high-$L$ states, especially since the collisional lifetime calculation cannot be trusted to better than an order of magnitude. The problem is, however, not very serious, since for most of the data, the homogeneous broadening is dominated by effects which do not involve the lifetime. As a check on the effect of the uncertainty in the lifetime related effects, some lines were taken several times with different laser intensities. Reproducibility of the fit using the same temperatures and line centers was excellent. Furthermore, an order of magnitude decrease in laser intensity would make many of the lines unobservable. Thus we are confident that the values we use for the lifetimes and saturation intensities do not significantly bias the results derived from the measurements.

#### 3. Other velocity-independent broadening mechanisms

The other velocity-independent mechanisms that contribute to the spectral line broadening and that

concern us are magnetic field inhomogeneities, electron beam-related Stark broadening, and long-term averaging effects including drifts in laser frequency.

The magnetic field inhomogeneity was measured for each transition using the NMR field probe. This inhomogeneity ranged between negligible to as much as ~50 G/cm for some transitions taken in an uncompensated magnet.

If we approximate the electron beam's $1.2 \times 1.0$ cm rectangular column of charge by a 1.2-cm-diameter cylindrical charge we can easily estimate the radial electric field. For typical operating conditions, this field is ~6 V/cm at the cylinder's surface and zero at its center. The effect of this field depends on the polarizability of the state and the magnetic field at which we are making the observation. The largest polarizability we observed was at ~70 kG where the motional Stark field of ~100 V/cm gives rise to a motional Stark shift of ~335 MHz while the Stark shift due to the electrons using the above surface field, is ~2 MHz. Varying the electron beam current between 1 and 3 mA showed no noticeable effect on the resonances other than improving the signal to noise. We did note a definite change in position and shape of the resonances when the current was increased above 10 mA. For almost all the data, the current was 3 mA.

The laser was repeatedly retuned to line center during the data averaging but due to the high gain mode of operation, it was measured to drift by ~±9 MHz. The field was checked prior to each sweep and was resettable to ±1 G.

In fitting the lines we combined all of the velocity-independent broadening mechanisms into a "nonlifetime homogeneous width", $\Delta B_h$, which varied from 10 to 25 G depending on the exact experimental conditions. The line fitting was not very sensitive to this number, and a change of a few gauss made very little difference in the zero-field results or the quality of the fit. In the fitting formula, the nonlifetime homogeneous width was simply added to the power-broadened lifetime width.

#### *4. Determination of gas temperature*

The data indicates that there is a systematic problem with the temperatures $T$, which enter into the line shape through $v_0$, required to fit the lines. Thus, it was important to independently establish the gas temperature. To determine experimentally the temperature, we repeated the observation[2] of a low-field $7\,^1S$-$9\,^1P$ transition. This resonance, (using the 10-$\mu$m R28 laser line) is at ~2 kG and has a negligibly small motional Stark shift. It can therefore be well fit with a Voigt profile. The fit required a temperature of 450 K and a homogeneous width of 15 G.

This higher than ambient temperature is presumably due to the gas passing over the hot (~900 °C) electron gun. The temperature varied slightly (±20 K) from time to time because data taken at different times used different electron guns which required slightly different temperatures for electron emission. We further believe that this is the correct temperature of the gas, since all of the $7\,^1S$-$9\,^1P$ data were fit assuming a temperature of ~450±20 K. As we shall see, the data fitting for the high-$L$ states required a wide range of temperatures between 250 and 600 K.

### B. Even-parity $m_L = 2$ transitions

The fitting of the data for these transitions was performed by using Eqs. (A19) and (A20) of the previous paper.[5] In our derivation of the line-shape function, we assumed the mixing of the $9\,^1P$ state to only be a function of atomic velocity and not vary over the spectral linewidth. However, as can be seen from Fig. 6, the admixture of $^1P$ character can at times vary rapidly with magnetic field. Thus we included this variation in our fitting program, by allowing the saturation intensity to be field dependent. The results of the fitting and the fitting parameters are listed in Table I. In the procedure used to fit the lines we identified the transitions by labeling them in terms of the zero-field angular momentum of their upper states. Thus R32L8 refers to the transition to the $L_0 = 8$ state ($n = 9$, $m_L = 2$) with the R32, 10-$\mu$m $CO_2$ laser line. Examples of such experimental spectra are shown in Figs. 7 and 8 along with their theoretical fits. Reasonable values of $B_0$ the resonance position for an atom at rest and $T$ were assumed in the initial attempt at fitting the data. Using the assumed $B_0$, the net magnetic field tuning rate for the transition was calculated. This is simply the difference in the tuning rates of the upper and lower state. The tuning rate of the upper state (high $L$) must be obtained from the matrix diagonalization of the magnetic Hamiltonian. The tuning rate of the $7\,^1S$ state is given to the desired accuracy by the second-order tuning coefficient. Using the assumed $B_0$ and the tuning rate the next step involved the calculation of the polarizability, $\alpha_L$, and $I/I_{so}$.

The values of $\alpha_L$ and $I/I_{so}$ used in the fitting of the various transitions are also listed in Table I. The numerical values listed for these quantities were calculated for a thermal velocity atom at the listed temperatures, $T$. The polarizability, $\alpha_L$, is listed in the column headed MSS (Motional Stark Shift) and is given in units of the number of gauss

TABLE I. Parameters used in the line fitting for the even-parity, $n = 9$ states.

| Label | $B_0$(kG) | $\Delta B_h$(G) | $T$ (K) | MSS (G) | $I/I_{SO}$ |
|---|---|---|---|---|---|
| R24$L$2 | 20.337 ± 0.007 | 28 | 375 | 29 | 0.27 |
| R26$L$2 | 33.200 ± 0.008 | 18 | 375 | 73 | 1.1 |
| R28$L$2A | 45.608 ± 0.015 | 23 | 425 | 172 | 3.74 |
| R28$L$2B | 45.608 ± 0.015 | 23 | 475 | 154 | 4.18 |
| R30$L$2A | 57.663 ± 0.015 | 23 | 375 | 239 | 8.37 |
| R30$L$2B | 57.658 ± 0.015 | 23 | 400 | 255 | 13.8 |
| R30$L$2C | 57.658 ± 0.020 | 23 | 375 | 239 | 0.125 |
| R32$L$2A | | 23 | 385 | 472 | 25.0 |
| R32$L$2B | 69.316 ± 0.010 | 23 | | | |
| R32$L$4 | 65.164 ± 0.010 | 15 | 325 | −5 | 0.032 |
| R32$L$6 | 64.787 ± 0.007 | 25 | 325 | −4 | 0.075 |
| R32$L$8 | 63.950 ± 0.005 | 10 | 250 | −3 | 0 |
| R34$L$4 | 77.316 ± 0.005 | 20 | 275 | −4 | 0.13 |
| R34$L$6 | 76.737 ± 0.005 | 18 | 275 | 0 | 4.69 |
| R34$L$8A | 75.537 ± 0.007 | 13 | 250 | 0 | 6.22 |
| R34$L$8B | 75.537 ± 0.007 | 13 | 250 | 0 | 2.21 |
| R34$L$8C | 75.531 ± 0.007 | 18 | 250 | 3 | 8.89 |
| R34$L$8D | 75.528 ± 0.007 | 13 | 250 | 2 | 8.29 |
| R38$L$6 | 99.662 ± 0.010 | 23 | 525 | −106 | 3.79 |
| R38$L$8 | 97.572 ± 0.008 | 23 | 600 | −87 | 5.81 |
| R40$L$6 | 110.595 ± 0.012 | 23 | 525 | −155 | 6.86 |
| R40$L$8 | 108.021 ± 0.008 | 23 | 425 | −70 | 2.83 |
| R42$L$4 | 122.677 ± 0.010 | 23 | 300 | −183 | 3.78 |
| R42$L$6 | $121.055^{+0.010}_{-0.015}$ | 13 | 450 | −194 | 3.87 |
| R42$L$8 | 118.122 ± 0.007 | 23 | 425 | −83 | 1.75 |

that is the resonance of an atom with velocity $v_0$ will shift due to the motional Stark effect at the given magnetic field. All of these quantities were then used as the input parameters in our line-shape computation. The parameters $B_0$ and $T$ were then varied and adjusted until a satisfactory (determined "by eye") fit was found.

For some resonances, e.g., R30L2A, R30L2B, R30L2C, there is more than one entry in Table I. This situation arises because the observations were made under different conditions, e.g., different laser power levels. The close agreement between the values of $B_0$ for the various independent fits under different conditions is further evidence for the accuracy of its determination. The systematic variation in the temperatures required to fit the lines is apparent in the table. An assumed temperature affects the data in two general ways; through the size of the Doppler shift and the size of the motional Stark shift suffered by the atoms. Thus in those cases where the MSE dominates the line shape one might be tempted to explain the "temperature problem" by questioning the polarizability calculation. One could increase

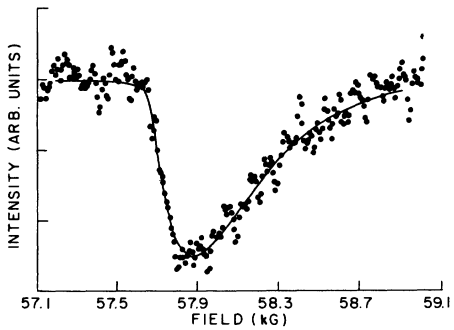


FIG. 7. Data and fit for the transition $7\,^1S$-$9\,^1D$ using the R30 laser line of the 10.6-$\mu$m branch with $B_0 = 57.658$ kG. The theoretical curve was obtained using the parameters listed in Table I for line R30L2B.

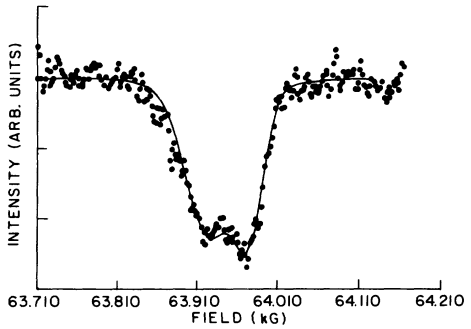


FIG. 8. Data and fit for the transition $7\,^1S$-$9\,^1$ ($L = 8$) using the R32 laser line of the 10.6-$\mu$m branch with $B_0 = 63.950$ kG. The theoretical curve was obtained using the parameters listed in Table I for line R32L8.

or decrease $\alpha_L$ and leave $T$ fixed at a reasonable value to arrive at the desired motional Stark shift. This procedure, however, cannot work in those cases where the motional Stark shift is very small and the line is essentially symmetric. These lines (such as the R32 and R34 $L_0=4,6,8$) could only be fit with essentially zero polarizability and thus clearly indicate that the problem lies in the assumption of a Maxwell-Boltzmann distribution or in the assumption of an equilibrium temperature characterizing all the states of an atom.

We are unable to quantitatively explain this difficulty, or even to identify with certainty the source of the problem. From the $7\,^1S$-$9\,^1P$ data the temperature was measured to be 450 K and the fit for that data implicitly contains in it the assumption of a Maxwell-Boltzmann velocity distribution. Since the high-$L$ data were also obtained from transitions originating in the same $7\,^1S$ state the peculiarity is clearly a property of the high-$L$ states.

It is interesting to note that no similar temperature problem is found in the $n=9$, high-$L$, odd-parity, $m=+1$ states (see Sec. IV C). A tentative explanation is to postulate that the true velocity distribution in our system is somewhat non-Maxwell-Boltzmann perhaps due to the restrained motion of the ionic core in the magnetic field. Since the high-$L$, even-parity transition line shapes are extremely sensitive to the tail (high velocity atoms) of the velocity distribution the anomaly is observable clearly only in these transitions. Both the $7\,^1S$-$9\,^1P$ and the high-$L$, odd-parity transitions have a different and much less velocity sensitive line shape and thus show no temperature problems.

There has been very little work bearing on such temperature effects. Theoretically, Derouard and Lombardi[52] have developed a model for angular momentum changing collisions for Rydberg atoms colliding with rare gases. This model is a simple semiclassical one however, and predicts no net deviation from a Maxwell-Boltzmann distribution. Experimental work with high-$L$ states is also lacking. The anticrossing experiment of Beyer and Kollath[35] is not a very sensitive test of the temperature and no temperature anomaly is reported. The work of Gallagher *et al.*[53] using microwaves to drive transitions to high-$L$ states in Na is likewise insensitive to the velocity distribution.

The temperature anomalies seem very systematic for transitions observed below about 90 kG (all the transitions to $L_0=2$ states are fit with ~375 K except for the R28 transition where there is probably some accidental mixing with a nearby triplet state, and all of the $L_0=4,6,8$ states, below the crossing with $9\,^1P$, are fit with 250–325 K). Above 90 kG however, the temperature problem is much more erratic. A possible explanation for the high-field erratic temperatures may be found by examining as an example the transitions driven by the R42 laser line. We were unable to find a consistent set of parameters that would fit the experimental line shape for the transition to the $L_0=2$ state. The difficulty arises for several reasons: (1) Around 120 kG the $L_0=2$ and $L_0=4$ states are very close, (2) the magnetic field is very large giving rise to a large motional Stark field, and (3) both states have ~35% $D$ character. These states can couple to each other through the $9\,^1P$, $m_L=1$ state via the motional Stark field. Thus, this coupling is strong and gives rise to terms of higher order in perturbation theory. By a rough calculation, we find that for the $L_0=2$ state at $B\approx 120$ kG the motional Stark shift for a $v_0$ atom decreases by about 40% from what is calculated in second-order perturbation theory.

We can reasonably postulate that the cause for the erratic behavior of the temperature required to fit the lines above 90 kG is really due to the inaccuracy of the polarizability calculation. The inaccuracy tends to increase the motional Stark shift for the $L_0=8$ state and decrease it for the $L_0=2$ states. For states with $L_0=4,6$, the effect is somewhere in between. This is indeed consistent with the data. This explanation, however, cannot apply to transitions at fields below ~80 kG because there are no states coupled strongly enough to the $9\,^1P$ to make higher order interactions important. For example, we have estimated the size of this effect for the $L_0=8$ and 6 states at 75 kG. This calculation reveals that higher order terms would decrease the motional Stark shift by only ~2% for the $L_0=8$ state which is negligible.

The values of the motional Stark shift needed to give the best fit to the remaining transition line shapes were in almost all cases consistent with the calculated values of $\alpha_L$. However, a couple of minor exceptions were found. For the R34, $L_0=6$ transition, the calculated motional Stark shift (for the fit temperature) is 7 G, while the line was fit with 0 G. Similarly, for the R34, $L_0=8$ transition, the calculated value is 13 G (at 250 K) while the line could be fit with, at most, 3 G. In percentage deviations these errors are enormous; however, in absolute terms an error of 7–10 G is not very large. We attribute these errors to the neglect of the triplet states, which under some circumstances can influence the singlet states, thus slightly increasing or decreasing the motional Stark shift of that state.

The transition at about 69 kG to the $L_0=2$ state driven by the R32 laser line is very broad (3 kG),

and with our present apparatus we could not obtain all of this transition in a single stabilized field sweep. Therefore a combination of broad unstabilized and a narrow stabilized sweep (labeled R32L2A and R32L2B in Table II) which included only the "sharp" side of the line was used in the line fitting. The transition to the $L_0=2$ state driven by the R34 laser line at about 81 kG is also very broad due to the close proximity of this state to the $9\,^1P$ state. In fact the motional Stark effect for this transition is so large that our perturbation theory can no longer be expected to work. Thus no attempt was made to fit this data.

The transitions driven by the 10-$\mu$m R36 laser line are completely unresolved. All these states are very close (within a few kG) to the $9\,^1P$ state so interpretation of this data would again be very difficult. No attempt was made to fit any of these transition line shapes. A similar problem occurs with transition driven by the 10-$\mu$m R38 laser line. The transitions to the $L_0=2$ and 4 are much too close to resolve. The transition to the $L_0=6$ state although partially resolved is still too close to $L_0=2$, 4 to allow a good fit. Thus we use only the R38 driven $L_0=8$ state for extrapolation back to zero field. The same problem occurs with the R40 transitions where only $L_0=8$ and $L_0=6$ are clearly resolved and analyzable.

It is important to point out that even with large widths and the uncertainties in temperature the values of $B_0$ we obtain from the spectral lines are quite reliable. $B_0$ is always determined by fitting the sharper side of the line, i.e., where these effects are small. The errors associated with $B_0$ as obtained from the line fitting of the forbidden transitions are larger than those associated with the $B_0$'s in Ref. 2. This occurs because here the motional Stark field significantly broadens the lines without adding any "sharp" feature. Spectral lines for allowed transitions, such as the $7\,^1S$-$9\,^1P$, can be drastically broadened but an extremely sharp edge is also formed in the spectral line. For lines associated with forbidden-type transitions no similar sharp feature arises. When lines are broadened to 2 kG, an uncertainty of 30 G in $B_0$ is therefore not unreasonable.

TABLE II. Parameters used in the line fitting for odd-parity, $n=9$ states.

| Label | $B_0$(kG) | $\Delta B_h$(G) | $T$ (K) | MSS (G) |
|---|---|---|---|---|
| R30L3 | 107.021±0.007 | 15 | 440 | −25 |
| R30L5 | 103.809±0.005 | 15 | 480 | −26 |
| R30L7 | 99.482±0.005 | 15 | 480 | −23 |
| R32L3 | 132.216±0.005 | 20 | 450 | −38 |
| R32L5 | 127.375±0.005 | 20 | 400 | −29 |
| R32L7 | 120.957±0.007 | 20 | 550 | −36 |

### C. Odd-parity, $m_L=1$ transitions

Fitting the spectral lines for the transitions from the $7\,^1S$ state to the $n=9$, $L$ odd, $m_L=1$ states of helium was done using Eq. (11) of Ref. 2. In comparison to the even-parity transitions, the fitting for these transitions was straightforward. The results of these fits are given in Table II. The motional Stark shifts for these transitions are quite small so the dominant broadening mechanism is the Doppler shift. As we have pointed out earlier, the odd-parity transition temperatures are consistent with our expectations based on the $7\,^1S$-$9\,^1P$ measurements.

### D. Extrapolation to zero magnetic field

From the values of $B_0$ obtained from the line fitting we are able to infer the zero-field energies of the high angular momentum states. The procedure is identical for both the even- and odd-parity states. The method used was to do a global least-squares fit to the $B_0$ values using the zero-field separations as independent variables. The calculated resonance positions are obtained from a diagonalization of the magnetic Hamiltonian, Eq. (1) of the previous paper.[5] Only the zero-field values were varied in the least-squares fitting. No attempt was made to vary the matrix elements of the magnetic Hamiltonian, as their values appear well established and such a procedure would have required excessive amounts of computer time.

The results of the least-squares fitting along with the data used to obtain the zero-field energies are presented in Table III. The $7\,^1S$-$9\,^1P$ energy separation[2] was subtracted from all the $7\,^1S$, high-$L$ separations. Since the error for that separation is five to ten times smaller than the standard errors obtained for the high-$L$ states the added error is insignificant.

The zero-field extrapolation resulted in rather large standard errors. These errors are 5–10 times worse than might be expected. The odd-parity states admittedly suffer from a lack of data points, but the ones that exist have very small residuals ($\leq$7 G). Yet the standard errors are ±0.0015 to ±0.0032 cm$^{-1}$ which correspond to ±30 to ±60 G (at 0.05 cm$^{-1}$/kG). The even-parity states have slightly better standard errors; from ±0.00055 to ±0.0019 cm$^{-1}$ which corresponds to ±6 to ±19 G (at 0.1 cm$^{-1}$/kG). These large errors are probably due to the insensitivity of the extrapolated energies to the energies of the states at high fields. Inspection of Figs. 2 and 3 shows that the separation of these states is primarily dependent on the magnetic field repulsions (which grows as $B^2$) and not their zero-field separations. The only real exception to this is the $9\,^1D$ state and the

TABLE III. Results of least-squares-fitting procedure for $n=9$, $L$ He states.

| Even-parity states | | | |
|---|---|---|---|
| $L$ | | $E(L)-E(9\,^1P)$ ($cm^{-1}$) | |
| 2 | | −4.243 82 ± 0.000 55 | |
| 4 | | −3.655 26 ± 0.001 31 | |
| 6 | | −3.624 44 ± 0.001 92 | |
| 8 | | −3.620 77 ± 0.001 32 | |
| Laser line | $L_0$ | Calculated field (kG) | Residuals (obs–calc) (G) |
| R24 | 2 | 20.332 | 5 |
| R26 | 2 | 33.187 | 13 |
| R28 | 2 | 45.624 | −16 |
| R30 | 2 | 57.662 | −2 |
| R32 | 2 | 69.323 | −7 |
| R32 | 4 | 65.180 | −16 |
| R32 | 6 | 64.797 | −10 |
| R32 | 8 | 63.964 | −14 |
| R34 | 4 | 77.314 | 3 |
| R34 | 6 | 76.735 | 2 |
| R34 | 8 | 75.533 | 4 |
| R38 | 8 | 97.566 | 6 |
| R40 | 6 | 110.570 | 25 |
| R40 | 8 | 108.027 | −6 |
| R42 | 4 | 122.665 | 2 |
| R42 | 6 | 121.063 | −8 |
| R42 | 8 | 118.113 | 9 |
| Odd-parity states | | | |
| $L$ | | $E(L)-E(9\,^1P)$ ($cm^{-1}$) | |
| 3 | | −3.746 00 ± 0.003 15 | |
| 5 | | −3.631 50 ± 0.001 55 | |
| 7 | | −3.621 60 ± 0.001 52 | |
| Laser line | $L_0$ | Calculated field (kG) | Residuals (obs–calc) (G) |
| R30 | 3 | 107.017 | 4 |
| R30 | 5 | 103.806 | 3 |
| R30 | 7 | 99.474 | 8 |
| R32 | 3 | 132.222 | −6 |
| R32 | 5 | 127.377 | −2 |
| R32 | 7 | 120.964 | −7 |

resulting standard error for this state is significantly better.

To obtain accurate zero-field energies for the observed states a slight modification of the results of the least-squares-fitting procedure, listed in Table III must be made. At high fields we observe these states in a complete Paschen-Bach limit, thus there is no interaction with triplet states. In extrapolating back to zero field, the numbers obtained would be the zero-field energies only in the absence of any interaction with triplet states. In the presence of such an interaction we can use the Breit-Bethe theory of relativistic fine structure to add in this repulsion and arrive at the true zero-field energies of the states. MacAdam and Wing[22] indicate that for $L \geq 4$ nonrelativistic contributions (i.e., exchange terms) are negligible and have shown that to very high accuracy the Breit-Bethe theory works quite well. Thus for the states $L \geq 4$ we adjust the extrapolated energies with the calculation of the displacement due to relativistic effects as given in Ref. 20. For $L=3$, exchange effects are important and must be included. From the $^{1,3}F$ splitting measured by MacAdam and Wing[22] for $n=10$–12, we extrapolate a value for $n=9$, which we use to determine the exchange integral. We then use this result in addition to Breit-Bethe theory to obtain the additional repulsion due to relativistic effects. The $^{1,3}D$ and $^{1,3}P$ separations are very large because of electrostatic effects and no corrections are necessary for these states. The final results for the $^1L=1$–8 zero-field energies appear in Table IV. In this table we arbitrarily set the zero-field energy of the $^1D$ state to zero, and also show the theoretical predictions of Deutsch,[31] which are based on polarization theory.

## V. DISCUSSION

In Table V our zero-field results are compared to measurements or predictions of MacAdam and

TABLE IV. Relative energies of singlet, $n=9$, $L$ states ($cm^{-1}$) and quantum defect $\delta$.

| $L$ | Energy expt [a] | Energy expt [b] | Theory [c] | $\delta$ |
|---|---|---|---|---|
| 1 | 4.2438 ± 0.000 59 | 3.6206 ± 0.0013 | | −0.012 053 2 ± 0.000 003 4 |
| 2 | 0 | −0.6232 ± 0.0014 | −0.562 | 0.002 07 ± 0.000 005 |
| 3 | 0.4984 ± 0.003 2 | −0.1248 ± 0.0034 | −0.119 | 0.000 42 ± 0.000 01 |
| 4 | 0.5892 ± 0.001 4 | −0.0340 ± 0.0019 | −0.032 | 0.000 113 ± 0.000 006 |
| 5 | 0.6124 ± 0.001 6 | −0.0102 ± 0.0020 | −0.011 | 0.000 036 ± 0.000 007 |
| 6 | 0.6195 ± 0.002 0 | −0.0037 ± 0.0023 | −0.004 | 0.000 012 ± 0.000 008 |
| 7 | 0.6223 ± 0.001 6 | −0.0009 ± 0.0020 | −0.001 | 0.000 003 ± 0.000 007 |
| 8 | 0.6232 ± 0.001 4 | 0 | 0 | |

[a] Referenced to $L=2$ at zero energy.
[b] Referenced to $L=8$ at zero energy.
[c] Reference 31.

TABLE V. Comparison with other experimental and derived results.

| States | Other results | | Present results |
|---|---|---|---|
| $^1P-{}^1D$ | 4.2452 | ±0.0001 [a] | 4.2438±0.00055 |
| $^1D-{}^1F$ | 0.49783 | ±0.0001 [b] | 0.4984±0.0032 |
| $^1F-{}^1G$ | 0.091 679 | ±0.000 003 [b] | 0.0908±0.0035 |
| $^1D-{}^1G$ | 0.590 311 | ±0.000 001 [b] | 0.5892±0.0014 |
| $^1D-L=3$ | 0.4989 | ±0.0053 [c] | 0.4984±0.0032 |
| $^1D-L=4$ | 0.5897 | ±0.0022 [c] | 0.5892±0.0014 |
| $^1D-L=5$ | 0.6145 | ±0.0020 [c] | 0.6124±0.0016 |
| $^1D-L=6$ | 0.621 | ±0.0027 [c] | 0.6195±0.0020 |
| $^1D-L=7$ | 0.6239 | ±0.0033 [c] | 0.6223±0.0016 |
| $^1D-L=8$ | | | 0.6232±0.0014 |

[a] Reference 21.
[b] Reference 22.
[c] Reference 35.

Wing[22] and measurements of Beyer and Kollath.[35] For all the transitions our measurements agree with the others within the experimental error. The only disagreement is our measured $^1P$-$^1D$ separation as compared to that predicted[22] for this separation. The predicted value is well outside (over two standard deviations) our experimental error. Since the prediction is based on some rather difficult measurements in the $n=16-18$ states, data in low $n=3$ and 4 states, and optical data for $n=6-10$ which has much lower precision, we believe our value to be correct. Further support for this conclusion can be arrived at by considering that our measurements of the $D$-$F$, $D$-$G$, $F$-$G$ separations depend strongly on the position of the $^1D$ energy, and that if we fix the $^1D$ energy at the predicted value of MacAdam *et al.*,[22] these separations would not agree with their more precisely determined intervals.

In Table IV we compared our measurements to the predictions of Deutsch.[31] To within his calculated precision the agreement is excellent for high-$L$ (>4) states. As $L$ decreases, the discrepancy gets quite large, as one would expect, since polarizability calculations are not expected to work at low-$L$ values (large core penetration). The adequacy of polarization theory for the high-$L$ states is evident. In addition if we assume that the $L=8$ state is completely hydrogenic (which it is within our experimental error) we can derive quantum defects for all the states with $L$ greater than 0. These are also listed in Table IV.

Overall the experiments and analysis presented in this paper represent a detailed study of a set of high angular momentum states in He. We have observed complete $L$ mixing by a magnetic field with about two orders of magnitude higher resolution than previous experimenters. We have measured the relative zero-field energies of the $n=9$, $L=1-8$ states of helium and found that our measurements do not always agree with previous measurements or predictions.

The discrepancy of our measured $n=9$, $^1P$-$^1D$ separation from the predicted value of MacAdam *et al.*[22] necessitates further work in $^1P$-$^1D$ separations either in the far infrared or using a method similar to that used in this work. Experiments at different $n$ values would also be valuable in yielding the small $n$ dependence of the He quantum defects.

## ACKNOWLEDGMENT

The work of R. P., M. R., and B. L. was supported by the National Science Foundation.

*Present address: Bell Laboratories, Holmdel, New Jersey 07733.
†Also Physics Dept., MIT.
‡Guest scientist at the Francis Bitter National Magnet Lab.

[1]M. Rosenbluh, T. A. Miller, D. M. Larson, and B. Lax, Phys. Rev. Lett. 39, 874 (1977).
[2]M. Rosenbluh, R. Panock, B. Lax, and T. A. Miller, Phys. Rev. A 18, 1103 (1978).
[3]G. C. Neuman, B. R. Zegarski, T. A. Miller, M. Rosenbluh, R. Panock, and B. Lax, Phys. Rev. A 18, 1464 (1978).
[4]R. Panock, M. Rosenbluh, B. Lax, and T. A. Miller, Phys. Rev. Lett. 42, 172 (1979).
[5]R. Panock, M. Rosenbluh, B. Lax, and T. A. Miller, Phys. Rev. A 22, 1041 (1980).
[6]T. A. Miller and R. S. Freund, Adv. Magn. Reson. 9, 49 (1979).
[7]J. W. Farley, K. B. MacAdam, and W. H. Wing, Phys. Rev. A 20, 1754 (1979).
[8]F. M. J. Pichanick, R. D. Swift, C. E. Johnson, and V. N. Hughes, Phys. Rev. 169, 55 (1968).
[9]S. A. Lewis, F. M. J. Pichanick, and V. W. Hughes, Phys. Rev. A 2, 86 (1970).
[10]A. Kponou, V. W. Hughes, C. E. Johnson, S. A. Lewis, and F. M. J. Pichanick, Phys. Rev. Lett. 26, 1613 (1971).
[11]T. H. Maiman and W. E. Lamb, Jr., Phys. Rev. 98, 1194 (1955).
[12]W. E. Lamb, Jr., Phys. Rev. 105, 559 (1957).
[13]W. E. Lamb, Jr. and T. H. Maiman, Phys. Rev. 105, 573 (1957).
[14]I. Wieder and W. E. Lamb, Phys. Rev. 107, 125 (1957).
[15]T. A. Miller and R. S. Freund, Phys. Rev. A 4, 81 (1971).
[16]T. A. Miller and R. S. Freund, Phys. Rev. A 5, 588 (1972).
[17]W. H. Wing and W. E. Lamb, Jr., Phys. Rev. Lett. 28,

265 (1972).
[18]W. E. Lamb, Jr., D. L. Mader, and W. H. Wing, in *Fundamental and Applied Laser Physics, Proceeding of the Esfahan Symposium*, edited by M. S. Feld, A. Javan, and N. A. Kurnit (Wiley, New York, 1973), pp. 523–528.
[19]W. H. Wing, Jr., K. R. Lea, and W. E. Lamb, Jr., in *Atomic Physics 3*, edited by S. J. Smith and G. K. Walters (Plenum, New York, 1973), pp. 119–141.
[20]K. B. MacAdam and W. H. Wing, Phys. Rev. A 12, 1464 (1975).
[21]K. B. MacAdam and W. H. Wing, Phys. Rev. A 13, 2163 (1976).
[22]K. B. MacAdam and W. H. Wing, Phys. Rev. A 15, 678 (1977).
[23]W. H. Wing and K. B. MacAdam, in *Progress in Atomic Spectroscopy*, edited by W. Hanle and H. Kleinpoppen (Plenum, New York, 1978), pp. 491–527.
[24]T. A. Miller, R. S. Freund, F. Tsai, T. J. Cook, and B. R. Zegarski, Phys. Rev. A 9, 2974 (1974).
[25]T. A. Miller, R. S. Freund, and B. R. Zegarski, Phys. Rev. A 11, 753 (1975).
[26]J. Derouard, R. Jost, M. Lombardi, T. A. Miller, and R. S. Freund, Phys. Rev. A 14, 1025 (1976).
[27]H. J. Beyer and K. J. Kollath, J. Phys. B 8, L326 (1975).
[28]H. J. Beyer and K. J. Kollath, J. Phys. B 9, 185 (1976).
[29]R. M. Parish and R. W. Mires, Phys. Rev. A 4, 2145 (1971).
[30]T. N. Chang and R. T. Poe, Phys. Rev. A 10, 1981 (1974).
[31]C. Deutsch, Phys. Rev. A 13, 2311 (1976).
[32]T. N. Chang and R. T. Poe, Phys. Rev. A 14, 11 (1976).
[33]D. R. Cok and S. R. Lundeen, Phys. Rev. A 19, 1830 (1979).
[34]See R. H. Garstang, Rep. Prog. Phys. 40, 105 (1977) for a review of work to that time.
[35]H. J. Beyer and K. J. Kollath, J. Phys. B 11, 979 (1978); and H. J. Beyer and H. Kleinpoppen, in *Progress in Atomic Spectroscopy-Methods and Applications*, edited by W. Hanle and H. Kleinpoppen (Plenum, New York, 1978).
[36]M. Rosenbluh, H. Le, R. Panock, B. Lax, and T. A. Miller (unpublished).
[37]C. D. Harper and M. D. Levenson, Opt. Commun. 20, 107 (1977).
[38]R. J. Fonck, F. L. Roesler, D. H. Tracy, K. T. Lu, F. S. Tomkins, and W. R. S. Garton, Phys. Rev. Lett. 39, 1513 (1977); 40, 201 (E) (1978).
[39]M. L. Zimmerman, J. C. Castro, and D. Kleppner, Phys. Rev. Lett. 40, 1083 (1978).
[40]R. J. Fonck, D. H. Tracy, D. Wright, and F. S. Tomkins, Phys. Rev. Lett. 40, 1366 (1978).
[41]K. T. Lu, F. S. Tomkins, and W. R. S. Garton, Proc. R. Soc. London Ser. A 364, 421 (1978).
[42]K. T. Lu, F. S. Tomkins, H. M. Crosswhite, and H. Crosswhite, Phys. Rev. Lett. 41, 1034 (1978).
[43]H. Crosswhite, U. Fano, K. T. Lu, and A. R. P. Rau, Phys. Rev. Lett. 42, 963 (1979).
[44]N. P. Economou, P. R. Freeman, and P. F. Liao, Phys. Rev. A 18, 2506 (1978).
[45]A. R. P. Rau, Phys. Rev. A 16, 613 (1977).
[46]U. Fano, Coloq. Int. C.N.R.S. 273, 127 (1977).
[47]A. F. Starace, J. Phys. B 6, 585 (1973).
[48]T. F. Gallagher, S. A. Edelstein, and R. M. Hill, Phys. Rev. Lett. 35, 644 (1975).
[49]R. S. Freund, T. A. Miller, B. R. Zegarski, R. Jost, M. Lombardi, and A. Dorelon, Chem. Phys. Lett. 51, 18 (1977).
[50]A. H. Gabriel and D. W. O. Heedle, Proc. R. Soc. London, Ser. A 258, 124 (1960).
[51]M. Rosenbluh, Ph.D. thesis, MIT, 1978 (unpublished).
[52]J. Derouard and M. Lombardi, J. Phys. B 11, 3878 (1978).
[53]T. F. Gallagher, R. M. Hill, and S. A. Edelstein, Phys. Rev. A 13, 1448 (1976); 14, 744 (1976).